



Neural computing in four spatial dimensions

Arturo Tozzi¹ · Muhammad Zubair Ahmad² · James F. Peters²Received: 20 July 2019 / Revised: 26 April 2020 / Accepted: 11 May 2020
© Springer Nature B.V. 2020

Abstract

Relationships among near set theory, shape maps and recent accounts of the Quantum Hall effect pave the way to neural networks computations performed in higher dimensions. We illustrate the operational procedure to build a real or artificial neural network able to detect, assess and quantify a fourth spatial dimension. We show how, starting from two-dimensional shapes embedded in a 2D topological charge pump, it is feasible to achieve the corresponding four-dimensional shapes, which encompass a larger amount of information. Synthesis of surface shape components, viewed topologically as shape descriptions in the form of feature vectors that vary over time, leads to a 4D view of cerebral activity. This novel, relatively straightforward architecture permits to increase the amount of available qubits in a fixed volume.

Keywords Hall effect · Oscillations · Fourth dimension · Brain · Neuronal network

Multidimensional approaches are a novel field of research, with a potential to provide insights into neural organization (Tozzi 2019). However, these approaches are technically demanding to cope with elusive multidimensional activities. The recent onset of datasets encompassing thousands of features has led to the development of novel tools, such as feature selection, to model the underlying high-dimensional settings of neurodata generation (Garcia et al. 2018). Despite feature selection techniques allow the reduction of the data dimensionality and improve algorithms' performance (Dmochowski et al. 2017), huge data volume makes learning tasks computationally demanding. Increasing features' quantity/complexity results in reduced computational efficiency of algorithms. Most of the algorithms in use, developed for neural datasets of small size, cannot cope with the emerging Big Data problems. Therefore,

novel tools are required to quantify multidimensional issues related to neuronal systems.

In quantum computing, quantum properties can be used to represent and structure data (stored in terms of qubits), providing an amount of information higher than the classical computers. Here we describe a novel neural computing tool that is able, starting from simple shapes traces encompassed in a two-dimensional lattice, to detect information from a fourth spatial dimension. We aim to transfer the framework of the quantum Hall effects provided by Lohse et al. (2018) to the realm of brain computing, to demonstrate the feasibility of a synthetic quantum network equipped with four spatial dimensions (plus time), instead of the classical three (plus time).

We will describe 4D neural computing in terms of a computational device able to cope with *shape maps*, i.e., shapes' assessment at various hierarchical levels of synthesis. At first, we will define the fundamental structure for neural maps construction; then we will provide the operational steps for achieving 4D neural computing. We will also show that shape maps provide an expanded view of the Borsuk–Ulam Theorem (Tozzi et al. 2017), which allows to increase the amount of available qubits.

✉ Arturo Tozzi
tozziarturo@libero.it; Arturo.Tozzi@unt.edu

Muhammad Zubair Ahmad
ahmadmz@myumanitoba.ca

James F. Peters
James.Peters3@umanitoba.ca

¹ Center for Nonlinear Science, University of North Texas,
1155 Union Circle, #311427, Denton, TX 76203-5017, USA

² Department of Electrical and Computer Engineering,
University of Manitoba, 75A Chancellor's Circle, Winnipeg,
MB R3T 5V6, Canada


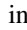
Introducing shape maps

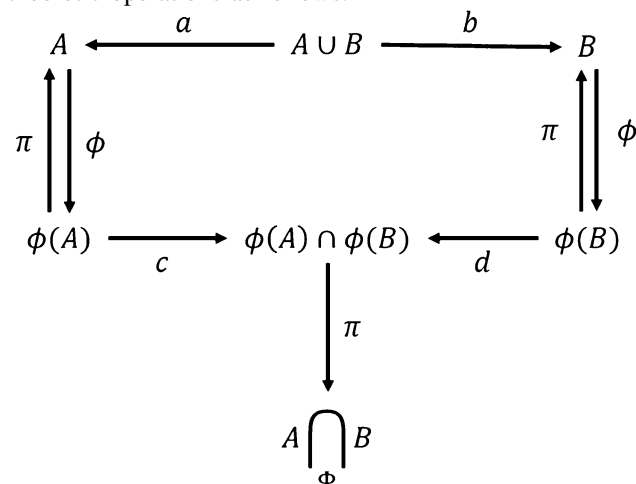
In near set theory, we consider a space K and a probe function $\phi : 2^K \rightarrow \mathbb{R}^n$ (Peters 2007, 2014). Given a small neighborhood $U \subset K$, we construct the fiber bundle $(K_\phi, K, \pi, \phi(U))$. Here, K_ϕ is termed the *glossa* (a set paired with description (Ahmad and Peters 2018)), i.e., a space where each $k \in K$ is paired with $\phi(k)$, due to the local trivialization property. This structure can be described as follows:

$$\phi(U) \rightarrow K_\phi \xrightarrow{\pi} K.$$

To define classical set theoretic operations incorporating description, we introduce the notion of *descriptive intersection* (Di Concilio et al. 2018). Let $A, B \subset K$ and $\phi : 2^K \rightarrow \mathbb{R}^n$. A descriptive intersection is defined as:

$$A \underset{\phi}{\cap} B = \{x \in A \cup B : \phi(x) \in \phi(A) \text{ and } \phi(x) \in \phi(B)\}.$$

Note that a descriptive intersection of sets A, B consists of all the elements. in either A or B , having the same description. In other words, sets A and B are close, provided there is at least one pair of elements a in A and b in B that are close descriptively. Implicit here are two forms of near sets, i.e., overlapping spatially near sets with  (figure 8 shape) and disjoint (non-overlapping) descriptively near sets containing shapes with the same description, e.g., $A = \{\square, \triangle\}$. $B = \{\sim, \triangle\}$ with shape  in common to A and B . In effect, members of the descriptive intersection of a pair of sets (e.g., neurons, brain signals) are a source of fibers and concomitant information in the form of closeness for what we call a topological charge pump. It follows that all the elements in $A \cap B$ are included in the descriptive intersection. We can represent this definition in terms of fiber bundle structure and classical set theoretic operations as follows:

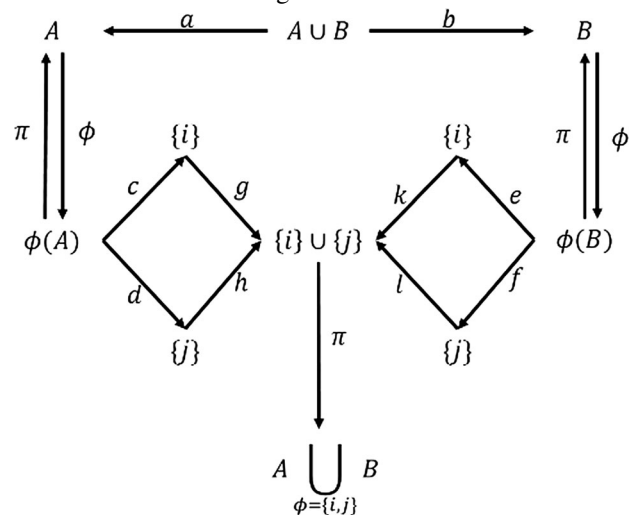


Note that the arrows are used here as connections in a topological sense, i.e., to establish descriptive intersection and union in fiber bundles.

Once established the notion of descriptive intersection, the next step is to define a descriptive union. Four different possible definitions have been discussed by Ahmad and Peters (2018): they consider either elements in $A \cup B$ (non-restrictive), or $A \cap B$ (restrictive), or few values of description (descriptive discriminatory), or all possible values (descriptive nondiscriminatory). Here we will evaluate just the *non-restrictive and descriptive discriminatory union*. Given $A, B \subset K$ and $\phi : 2^K \rightarrow \mathbb{R}^n$, non-restrictive and descriptive discriminatory union is described as follows:

$$A \underset{\phi=\{i,j\}}{\cup} B = \{x \in A \cup B : \phi(x) = i \text{ or } \phi(x) = j\}.$$

A non-restrictive and descriptive discriminatory union of sets A, B consists of all the elements of A and B that have matching description feature values $\{i, j\}$, with features such as shape energy and mass, decided a priori. A more detailed account of the properties of this union is given in Ahmad and Peters (2018). In terms of classical set theoretic operations and fiber bundles, the latter definition can be described in the following terms:



Shapes in terms of synthesis

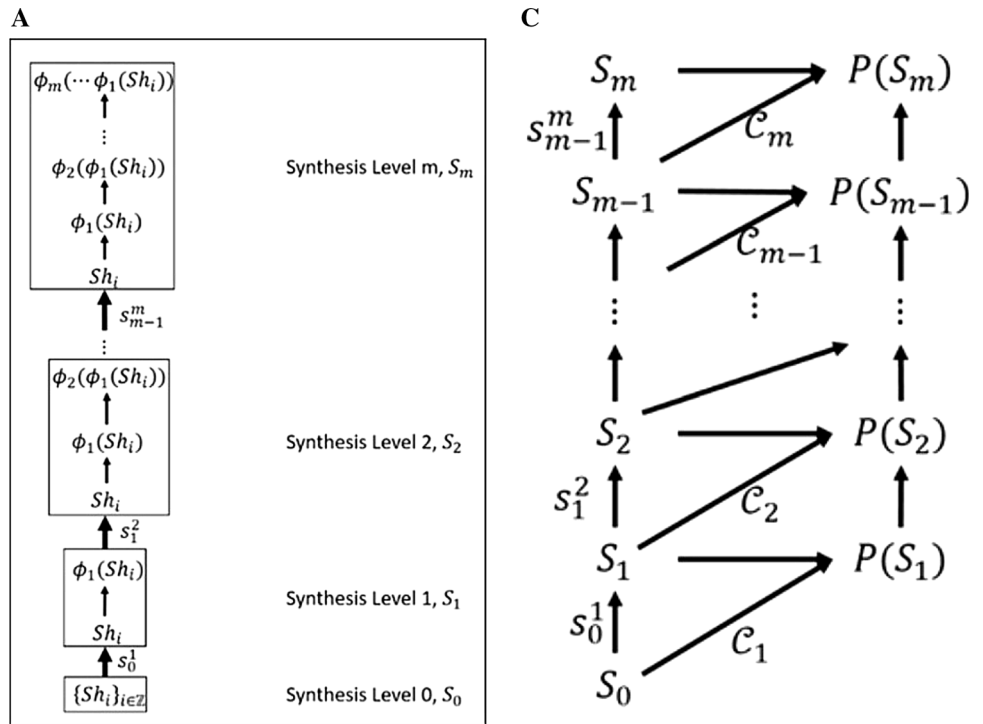
The next step is to define representation of a shape as a synthesis. We begin with a set of shapes $\{Sh_i\}_{i \in \mathbb{Z}}$ with no description attached to them. For simplicity, we assume them as embedded in a 2-dimensional space. This set of shapes is said to be at synthesis level 0, which is represented as S_0 . To attach description to these shapes, we use a probe function $\phi_1 : 2^{S_0} \rightarrow \mathbb{R}^n$ at level 0 and achieve a gloss presented as $\{Sh_i \rightarrow \phi_1(Sh_i)\}_{i \in \mathbb{Z}}$, standing for the synthesis

level 1 or S_1 . In other words, each shape synthesis spirals upward to more informative views of each shape and geometrically is a vortex with a shape at its center (level 0). We move onto the next level of synthesis, attaching another description to the one already attached in S_1 . Thus, S_2 is constructed using a probe function $\phi_2 : 2^{S_1} \rightarrow \mathbb{R}^n$. The corresponding glossa can be represented as $\{Sh_i \rightarrow \phi_1(Sh_i) \rightarrow \phi_2(\phi_1(Sh_i))\}_{i \in \mathbb{Z}}$. We generalize for the m th synthesis level S_m , using the probe function $\phi_m : 2^{S_m} \rightarrow \mathbb{R}^n$. This means that the glossa at S_m can be written as $\{Sh_i \rightarrow \phi_1(Sh_i) \rightarrow \dots \rightarrow \phi_{m-1}(\dots \phi_1(Sh_i)) \rightarrow \phi_m(\phi_{m-1} \dots \phi_1(Sh_i))\}_{i \in \mathbb{Z}}$. In sum, we define a family of functions that can be collectively termed as shape maps.

Let $s_i^{i+1} : S_i \rightarrow S_{i+1}$, be a map between the synthesis levels, then for a shape representation with m synthesis levels the shape maps are $\mathbb{S}_m = \{s_i^{i+1}\}_{i=1,2,\dots,m-1}$.

Figure 1a shows a shape map encompassing different levels of synthesis. The shapes Sh_i , exist at S_0 the zeroth level of synthesis. At S_1 , descriptions are attached to each shape with the help of a probe function ϕ_1 . At the next level of synthesis, a description is attached to the description of each of the objects by ϕ_2 . Similarly, increasing the levels of synthesis, we increase the number of descriptions until, at S_n , a description is attached to the previous level using ϕ_n . At the highest level, the

Fig. 1 Topological steps of shape maps construction. **a** Shape maps with n-levels of synthesis. **b** Shape maps lead to shapes clustered and glued together using descriptive intersection. **c** Shape description diagram for m-synthesis levels. See text for further details. The arrows are used here as topological steps of shape maps constructions



description can be written as a composition of maps $\phi_n(\phi_{n-1} \cdots \phi_1(Sh_i))$.

Once achieved shapes representation with the desired level of synthesis, we need to “organize” them according to a general description throughout all the levels. By “organizing” we mean clustering the shapes into sets based on some similarity criterion. Here the previously described near set paradigm comes into play. For this purpose, the descriptive intersection (Di Concilio et al. 2018) and the non-restrictive and descriptive discriminatory union (Ahmad and Peters 2018) are used. It is noteworthy there just one descriptive intersection is feasible, while the number of non-restrictive and descriptive discriminatory union depends on the number of pairs of descriptions $\{i, j\}$ selected a priori. We have set of descriptive set theoretic operators for each S_m . Let us represent this set at synthesis level j as:

$$\mathcal{O}^j = \left\{ \bigcap_{\Phi} \left\{ \bigcup_{\phi=A_i \in A} \right\}_{i \in \mathbb{Z}} \right\},$$

where $A = \{x \in 2^{\text{Codomain}(\phi_j)} : |x| = 2\}$.

In this set, we achieve both descriptive intersection and a selection of the possible non-restrictive and descriptive discriminatory unions. Further, if we take into account any of these operators for S_i , the synthesis assesses the descriptions attached at S_i and provides again the elements of the S_{i-1} level. This is clear from the arrow diagrams illustrated in Fig. 1a, which show how the descriptive set theoretic operations return the elements in the base space K , rather than the ones in the glossa K_{Φ} . We assume that each of the operators in \mathcal{O}^j can be used for a single set, instead of canonical binary operator. The same applies for the descriptive union in which all the elements with a priori decided descriptions are returned. We define a family of maps, which clusters the elements in S_i based on the application of operators in \mathcal{O}^i :

$$C_i = \left\{ c_j^i = s_{i-1}^i \left(\mathcal{O}_j^i(S_{i-1}) \right) \right\}_{j=1,2,\dots,|\mathcal{O}^i|},$$

where \mathcal{O}_j^i is the j th element of the set \mathcal{O}^i .

This map clusters the elements in S_i based on some similarity measure. If we consider the non-restrictive and descriptive discriminatory union with $\phi = \{i, j\}$ as the similarity measure, then it results in clustering all the shapes with description value of either i or j . Every operator in \mathcal{O}^i results in a different cluster (set) of S_i elements. Because each $c_j^i : S_{i-1} \rightarrow S_i$, their union to form C_i results in a new space $P(S_i)$, built by clustering the S_i elements. Hence, we can represent this as $C_i : S_{i-1} \rightarrow P(S_i)$. An example of this map is illustrated in Fig. 1b. This Figure also illustrates the beginning of a hyper Borsuk–Ulam

Theorem (Borsuk 1957–1958; Matoušek 2003; Tozzi and Peters 2016a). The introduction of a hyper-BUT paves the way to techniques for shape detection, “bunching” (clustering), classification, building (disparate shapes are synthesized to form new shapes for future reference), and shape analysis in a high-dimensional space (Tozzi and Peters 2016a, b). Shape building, also called bulk building, allows new shapes to be achieved. The hierarchical view of shape maps leads to two forms of synthesis, namely, shape-gluing (descriptive intersection) and shape agglomeration (descriptive union). We define another family of maps for synthesis level m represented as $\mathfrak{C}_m = \{C_i\}_{i=1,2,\dots,m}$, termed *clustering maps*. This allows to build a diagram termed *shape description diagram*, illustrated in Fig. 1c.

A tool from theoretical physics

Here we ask: is it feasible to assess and quantify how oscillations may generate multidimensional computations? More specifically, is it feasible to build a real or an artificial oscillatory network able to simulate an otherwise undetectable fourth spatial dimension? The answer is affirmative. Recent experimental findings describe a technique that throws an operational bridge between theoretical physics and quantum computing. At first, we explore the “Hall effect” (Hall 1879) observed in 2D systems with low temperatures and strong magnetic fields in which conductance σ map to quantized values defined by

$$\sigma = \nu \frac{e^2}{h}, \quad e = \text{charge}, \quad h = 6.6 \times 10^{-34} \text{ kg m}^2/\text{s}, \quad \nu = \text{filling factor},$$

i.e., the production of potential difference transverse to electric current, upon application of a magnetic field perpendicular to current.

Magnetic fields with the proper angulation are able to bend electric rays. A comparable phenomenon, called “quantum Hall effect”, occurs in quantum dynamics (Novoselov et al. 2007). An electric charge sandwiched between two surfaces behaves like a two-dimensional material: when this material is cooled down to near absolute-zero temperature and subjected to a strong magnetic field, the amount that it can conduct becomes “quantized”, leading to the so-called quantum Hall effect (Tozzi 2019). This puzzling phenomenon is easily explained, if we take into account that it occurs in four, instead of the canonical three, spatial dimensions (Zhang and Hu 2001; Kraus et al. 2013; Zilberberg et al. 2018). Lohse et al. (2018) found a (relatively) simple way to probe four-dimensional quantum physical phenomena, starting from an artificial, two-dimensional dynamic system, a superlattice termed “2D topological charge pump”. The light flowing through the

two-dimensional superlattice behaves according to the predictions of the four-dimensional quantum Hall effect. The Authors provided a two-dimensional waveguide equipped with patterns acting as manifestations of higher-dimensional coordinates: in operational terms, they built a 2D lattice consisting of superlattices along the x and y axes.

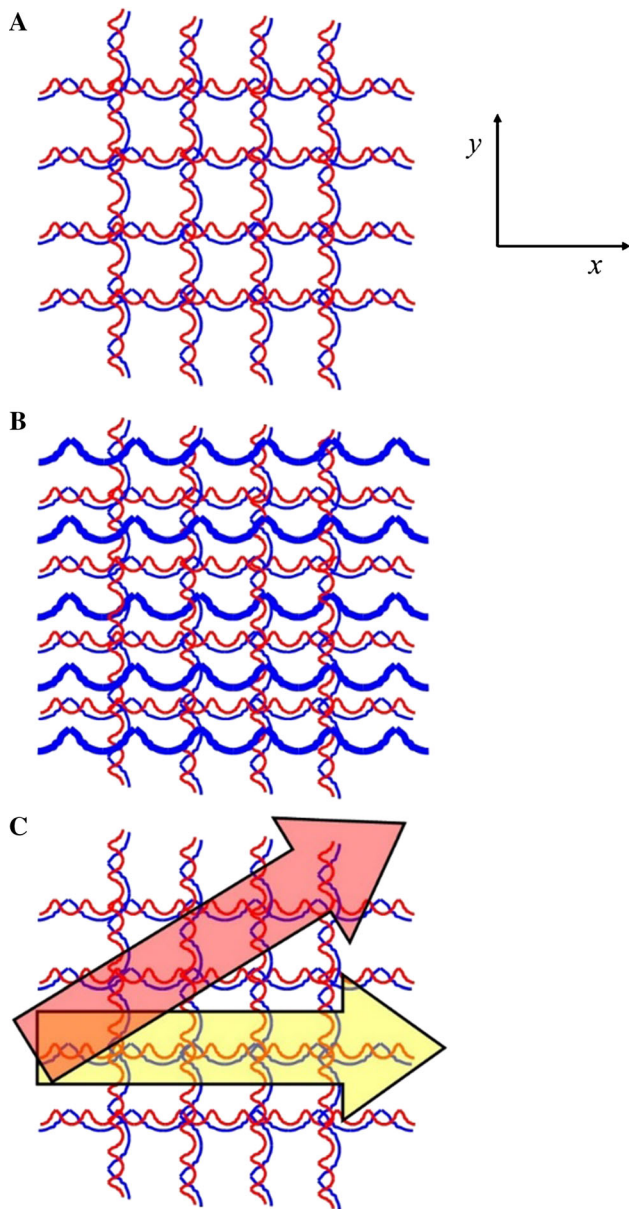


Fig. 2 4D physical activities on a 2D superlattice, according to Lohse et al. (2018). **a** Illustrates a topological lattice with two waves of different wavelength (red and blue thin lines). **b** Depicts a third wave (blue thick line) with the proper wavelength and angulation (not shown here) superimposed to the lattice along the x direction. The required angulation of the third wave might also be achieved by tilting the lattice. **c** The superimposition of the three waves gives rise to two different paths: a 2D linear one along the x axis (yellow arrow), and a nonlinear 4D one along the y axis (red arrow). (Color figure online) Modified from Tozzi (2019)

Each superlattice is achieved by superimposing two standing waves of different wavelength (Fig. 2a). When a third wave is introduced along the x direction, this corresponds to tilting the long lattice along a one-dimensional path shadowing the axis x , carefully choosing the proper inclination (Fig. 2b). Lohse et al. (2018) and Zilberberg et al. (2018) provided the proper measures (e.g., angles, equations) to detect the 4D spacetime quantum Hall effect. Their procedure on 2D topological charge pumps allows the achievement of dynamics along the y axis that are equivalent to movements in four spatial dimensions. In effect, shape vectors (σ, e, v, t) have components that describe time-varying shapes relative to the changing temporal (spacetime) component t . They lead to two different responses: a linear one (two-dimensional response with fixed v) along the axis x and a nonlinear one (four-dimensional response with time-varying σ relative to e, v) (Fig. 2c). In sum, the Authors provide a technique which describes quantum dynamics in terms of pure oscillations. Here we ask: could such procedure be transferred, with the due corrections, to quantum computing, in order to build a spatial four-dimensional device where quantum computational operations might take place?

Neural computations in the form of shape maps

In the previous paragraph, we showed that Lohse et al.'s (2018) approach, i.e., a 2D topological charge pump, holds true for the assessment of the unusual multidimensional phenomenon occurring in quantum dynamics' Hall effect. Here we aim to show how, with the proper amendments, their four-dimensional- apparatus could be also used to build, assess and quantify a further spatial dimension of neural networks endowed in two-dimensional lattices. In other terms, our aim is to explore 4D shapes using 2D functional lattices, where the constructing basis in the x and the y dimensions are superlattices, i.e., periodic layered structures derived from the superposition of two stationary waves of different wavelengths. Our goal is to correlate shape maps to Lohse' et al.'s 2D lattice oscillations, the latter standing for the S_0 at the 0th level of synthesis (Fig. 3, lowest part). The entire topological pump stands for the space K , while its horizontal and vertical oscillations stand, respectively, for $A, B \subset K$. The topological pump's phase φ_x (which is the pump parameter, achieved when pumping is performed by moving the long lattice along x) stands for the probe function φ_1 displayed in Fig. 1a. The topological pump's phase φ_y (which stands for a transverse superlattice phase that depends linearly on x , and which varies with φ_x changes) stands for the probe function φ_2 . Note that φ_x lies at the S_1 level of synthesis, while φ_y at the S_2 level. In sum, when φ_x is modified, we achieve changes in φ_y , which lead to a quantized non-

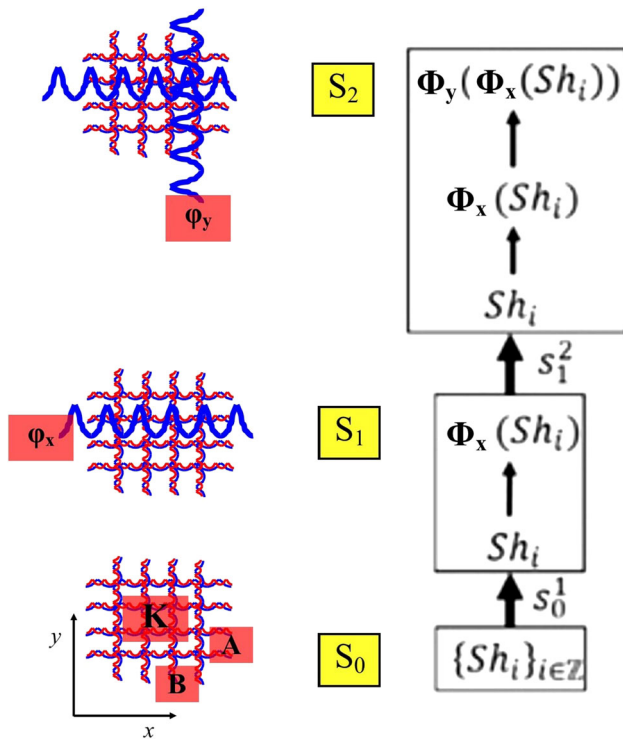


Fig. 3 Near set theory's and shape maps' lexicon can be used to describe the operations taking place on the 2D topological charge pump too. The yellow squares describe the levels of synthesis, while the red ones the near set theory's counterparts of the Lohse et al.'s lattice

linear response along y : such nonlinear response stands for the four-dimensional features in the topological space K . Note that, when an adiabatic pump cycle of the 2D topological charge pump is performed (Fig. 4), we achieve periodic modulation along closed trajectories, both on the horizontal and vertical plane (curves φ_x and φ_y in the upper part of the Fig. 4). In a full pump cycle, these closed trajectories cover a closed surface which lies in the 4D parameter space (middle part of Fig. 4). Our model allows the assessment of antipodal points in higher dimensions, due to the hyper-BUT dictates (Fig. 4, lower part). When evaluating 2D signals in 4D phase spaces, we achieve a multidimensional structure equipped with antipodal features with matching description.

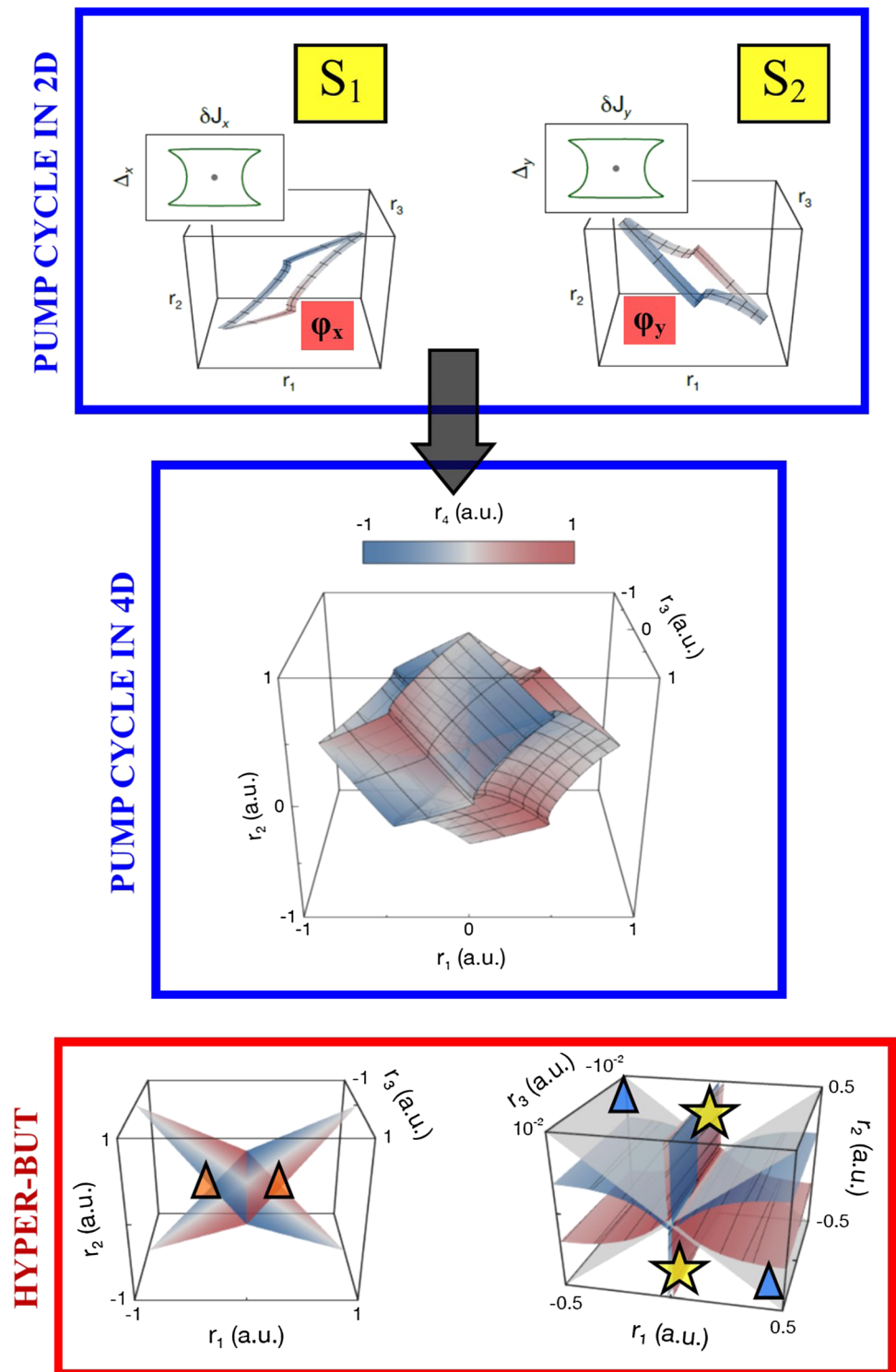
Conclusions

The benefits in using near sets in biomedical signal analysis, camouflage detection, human pattern recognition, cellular division trails, zero-shot recognition and visual pattern classification are clearly recognized in the literature. Linking these developments with our unconventional combination of disciplines in network science and

mathematics, we proposed a new form of neural computation using four spatial dimensions and sketch the preliminary theoretical steps to detect, assess and quantify a fourth spatial dimension using a neural network. In particular, we aimed to transfer the framework of the quantum Hall effect provided by Lohse et al. (2018) to the realm of neural computation, in order to: a) describe real multi-dimensional brain dynamics and b) demonstrate the feasibility of a synthetic network equipped with four spatial dimensions (plus time), instead of the classical three (plus time). We provided the theoretical apparatus to link two-dimensional topological charge pump to topological shape maps, achieving neural computing in four spatial dimensions. Indeed, working on a properly manipulated two-dimensional quantum lattice such as the topological charge pump, it is feasible to build a transverse oscillation standing for the whole system's four-dimensional component. We showed how the superimposition of waves of different frequency and orientation produces the required superlattice's functional reticulum. When the latter is crossed by other waves of different frequency along its x axis, both (two-dimensional) linear and (four-dimensional) nonlinear dynamics are accomplished. The superimposition of the proper waves gives rise to two quantifiable and assessable different motions: a linear one along the x axis, and a nonlinear one along the y axis. The oscillatory response along the y axis stands for the artificial network's component displaying the fourth spatial dimension.

The question is: why might scientist perform computations in four spatial dimensions, instead of the canonical three? How can real information be detected through a multidimensional apparatus? How much could neural computing profit from operations taking place in higher dimensions? The use of abstract mathematical language in multi-dimensions is justified if it helps to simplify our available techniques in neuroscience or design new applications (e.g., neurotechnology or neurodata tools). This might contribute to improve, for example, automatic classification of internal mental states during bistable perception (Sen et al. 2020), connectivity-based features of EEG signals for object recognition (Tafreshi et al. 2019), uncertainty removal in neural networks (Tozzi and Peters 2020). In Fig. 5, we provided an additional effort to simplify the very abstract concepts of high dimensional topology and to highlight their efficacy. We started from a three-dimensional network embedded in a convex manifold, where the quantum Hall effect is re-used for computational purposes (Fig. 5a). In operational terms, the network in Fig. 5a of specific oscillatory interactions in superlattices might be used also to assess more conventional neural network architectures, such as, e.g., manifolds representing electrophysiological thresholds of groups oscillating neurons already formulated in four dimensions

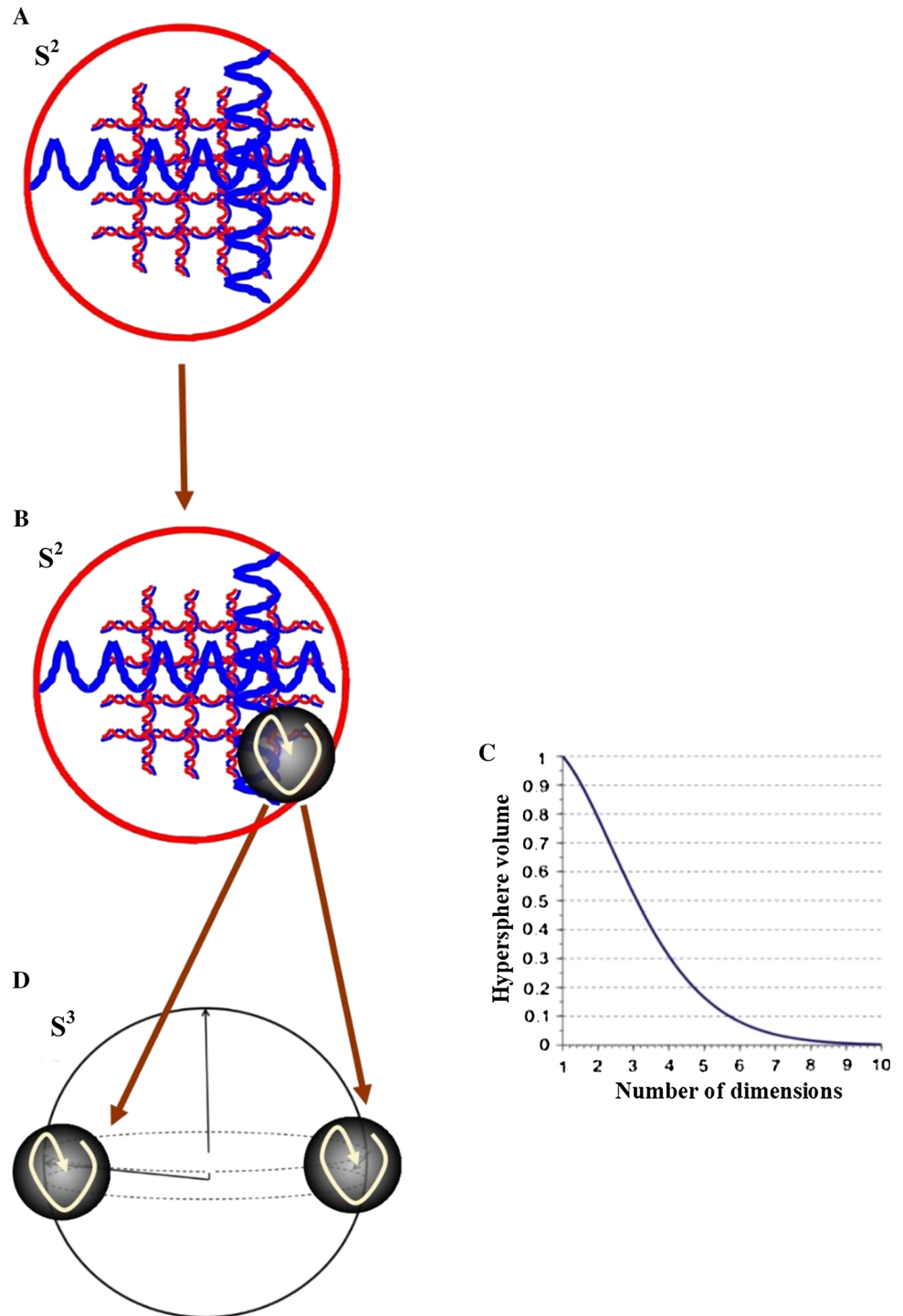
Fig. 4 Adiabatic pump cycle in different dimensions. Note that the paths in 2D give rise to a multifaceted manifold in 4D. The lower part of the Figure (embedded in a red square) illustrates how the Borsuk–Ulam theorem holds true for the 2D topological charge pump. Indeed, inside the transformed parameter space where singularities correspond to planes that touch at the origin, it is easy to detect several antipodal points with matching description (green and blue triangles, yellow stars). See Lohse et al. (2018) for further details and the legenda of the plots depicted here. (Color figure online)



(Izhikevich 2010), or spiking neural network models of mental imagery (Riley and Davies 2020), or neurocomputational models of semantic memory (Ursino et al. 2018). In our framework, fast and slow oscillations computing concepts of sets (e.g., union, intersection) may stand for both classes or operations in near set theory. The same

equivalence rules hold between classical set-theory and neural networks (e.g., like the classical McCulloch-Pits models) and between near sets and fiber bundles in 4 spatial dimensions. Once achieved an output signal (a shape) in three dimensions (Fig. 5b), we projected it to a four-dimensional hypersphere (Fig. 5d). This approach

Fig. 5 A simplified sketch of the suggested four-dimensional network. The Quantum Hall effect explains how a high-level description of a neural network could detect very general forms of information from a SPATIAL fourth dimension. **a** Three dimensional appearance of neuro-oscillatory activity in a Quantum Hall effect context. Different waves in the neural network superimpose according to the dictates of near sets symbols. An output (the shape in **b**) is produced in the three-dimensional manifold and is projected to a four-dimensional manifold in **d**, where, counterintuitively (**b**), a bigger amount of information can be stored in smaller amount of space



allows us to use projections and fiber bundles to make geometrical sense of extra “spatial” dimensions, so that we can move along an internal direction without carrying us away from the particular space–time point at which we are situated. This might explain fiber-independent coactivation of opposite fMRI activity, as suggested by Tozzi and Peters (2016a). In particular, when projecting qbits (a shape can be described in terms of qbits) from lower to higher

dimensions, their number increases (Fig. 5d), due to the dictates of the recently-developed variants of the Borsuk–Ulam theorem (Tozzi and Peters 2019). The shape projection from three to four spatial dimensions allows us to achieve TWO shapes with matching description, because the mappings takes place one dimensions higher. This means that a four-dimensional quantum computer amplifies the message, but does not require increases in phase

space's volume: indeed, going in higher dimensions, the manifold volume does not increase, while the information does (Fig. 5c) (Tozzi and Peters 2019). In other words, the interaction among different waves produces a novel functional dimension, i.e., a higher dimensional phase space where computational operations take place more efficiently at the same energetic cost.

To provide a theoretical operational example, in a visual two-dimensional scene the presence of the shape causes a deformation in two-dimensional topological charge pumps. The resulting four-dimensional wave represents neurons firing in different sections of the brain (Don et al. 2020) and a corresponding computer's response to the introduction of object shape parameters (geometry, feature vectors) in its oscillatory lattice. Therefore, four-dimensional oscillation is the main feature that leads to multiple shape vectors, i.e., each four-dimensional oscillation results in a corresponding shape description. Further, shape feature vector components have the x and y axes that can be arranged in varying orientations according to different required shape reconstructions, making it possible to achieve an increase in discriminatory power and detectable features. The last, but not the least, different neuronal activities might exhibit different four-dimensional hidden components, that, once detected, could be experimentally assessed and quantified.

References

- Ahmad MZ, Peters JF (2018) Descriptive unions. A fibre bundle characterization of the union of descriptively near sets, arXiv:1811.11129
- Borsuk K (1957–1958) Concerning the classification of topological spaces from the standpoint of the theory of retracts. *XLVI*:177–190
- Di Concilio A, Guadagni C, Peters JF, Ramanna S (2018) Descriptive proximities. Properties and interplay between classical proximities and overlap. *Math Comput Sci* 12(1):91–106. <https://doi.org/10.1007/s11786-017.0328-y>
- Dmochowski JP, Ki JJ, DeGuzman P, Sajda P, Parra LC (2017) Extracting multidimensional stimulus-response correlations using hybrid encoding-decoding of neural activity. *Neuroimage*. <https://doi.org/10.1016/j.neuroimage.2017.05.037>
- Don A, Peters JF, Ramanna S, Tozzi A (2020) Topological view of flows inside the BOLD spontaneous activity of the human brain. *Front Comput Neurosci*. <https://doi.org/10.3389/fncom.2020.00034>
- Garcia JO, Ashourvan A, Muldoon SF, Vettel J, Bassett DS (2018) Applications of community detection techniques to brain graphs: algorithmic considerations and implications for neural function. *Proc IEEE*. <https://doi.org/10.1109/jproc.2017.2786710>
- Hall E (1879) On a new action of the magnet on electric currents. *Am J Math* 2(3):287–292. <https://doi.org/10.2307/2369245>
- Izhikevich EM (2010) *Dynamical systems in neuroscience—the geometry of excitability and bursting*. ISBN: 9780262514200
- Kraus YE, Ringel Z, Zilberberg O (2013) Four-dimensional quantum Hall effect in a two-dimensional quasicrystal. *Phys Rev Lett* 111:226401
- Lohse M, Schweizer C, Price HM, Zilberberg O, Bloch I (2018) Exploring 4D quantum Hall physics with a 2D topological charge pump. *Nature* 553:55–58. <https://doi.org/10.1038/nature25000>
- Matoušek J (2003) *Using the Borsuk–Ulam theorem. Lectures on topological methods in combinatorics and geometry*. Springer, Berlin
- Novoselov KS, Jiang Z, Zhang Y, Morozov SV, Stormer HL et al (2007) Room-temperature quantum Hall effect in graphene. *Science* 315(5817):1379
- Peters JF (2007) Near sets. Special theory about nearness of objects. *Fundam Inf* 75(1–4):407–433
- Peters JF (2014) Topology of digital images. Visual pattern discovery in proximity spaces. In: *Intelligent systems reference library*. Springer, Berlin, pp 1–342, vol 63. ISBN 978-3-642-53844-5. <https://doi.org/10.1007/978-3-642-53845-2>
- Riley SN, Davies J (2020) A spiking neural network model of spatial and visual mental imagery. *Cogn Neurodyn* 14:239–251. <https://doi.org/10.1007/s11571-019-09566-5>
- Sen S, Daimi SN, Watanabe K et al (2020) Switch or stay? Automatic classification of internal mental states in bistable perception. *Cogn Neurodyn* 14:95–113. <https://doi.org/10.1007/s11571-019-09548-7>
- Tafreshi TF, Daliri MR, Ghodousi M (2019) Functional and effective connectivity based features of EEG signals for object recognition. *Cogn Neurodyn* 13:555–566. <https://doi.org/10.1007/s11571-019-09556-7>
- Tozzi A (2019) The multidimensional brain. *Phys Life Rev*. <https://doi.org/10.1016/j.pprev.2018.12.004> (in press)
- Tozzi A, Peters JF (2016a) Towards a fourth spatial dimension of brain activity. *Cogn Neurodyn* 10(3):189–199. <https://doi.org/10.1007/s11571-016-9379-z>
- Tozzi A, Peters JF (2016b) A topological approach unveils system invariances and broken symmetries in the brain. *J Neurosci Res* 94(5):351–365. <https://doi.org/10.1002/jnr.23720>
- Tozzi A, Peters JF (2019) The Borsuk–Ulam theorem solves the curse of dimensionality: comment on “the unreasonable effectiveness of small neural ensembles in high-dimensional brain” by Alexander N. Gorban et al. *Phys Life Rev*. <https://doi.org/10.1016/j.pprev.2019.04.008>
- Tozzi A, Peters JF (2020) Removing uncertainty in neural networks. *Cogn Neurodyn*. <https://doi.org/10.1007/s11571-020-09574-w>
- Tozzi A, Peters JF, Fingelkurts AA, Fingelkurts AA, Marijuán PC (2017) Topodynamics of metastable brains. *Phys Life Rev* 21:1–20. <https://doi.org/10.1016/j.pprev.2017.03.001>
- Ursino M, Cuppini C, Cappa SF et al (2018) A feature-based neurocomputational model of semantic memory. *Cogn Neurodyn* 12:525–547. <https://doi.org/10.1007/s11571-018-9494-0>
- Zhang S-C, Hu J (2001) A four-dimensional generalization of the quantum Hall effect. *Science* 294:823–828
- Zilberberg O, Huang S, Guglielmon J, Wang M, Chen KP et al (2018) Photonic topological boundary pumping as a probe of 4D quantum Hall physics. *Nature* 553(7686):59–62. <https://doi.org/10.1038/nature25011>

Publisher's Note Springer Nature remains neutral with regard to jurisdictional claims in published maps and institutional affiliations.